

## STATE DIAGRAM OF A PERPENDICULAR POLARIZER - SAF FREE-LAYER SPINTORQUE OSCILLATOR

I. FIRASTRAU<sup>a\*</sup>, U. EBELS<sup>b</sup>, D. GUSAKOVA<sup>b</sup>, M.C. CYRILLE<sup>c</sup>,  
C. B. CIZMAS<sup>a</sup>, L.D. BUDA-PREJBEANU<sup>b,d</sup>

<sup>a</sup>Transilvania University of Brasov, 29 Bld. Eroilor, 500036 Brasov, Romania

<sup>b</sup>SPINTEC (UMR8191 CEA/CNRS/UJF), CEA Grenoble, INAC, 38054 Grenoble, France

<sup>c</sup>CEA-LETI, MINATEC, DRT/LETI/DIHS, 17 rue des Martyrs, 38054 Grenoble, France

<sup>d</sup>Grenoble INP, 46, Avenue Félix Viallet, 38031 Grenoble Cedex 1, France

Wit is numerically investigated by using a macrospin approach the magnetization dynamics of a synthetic antiferromagnet (SAF) as a function of an injected spin polarized current and an applied magnetic field. The current is spin-polarized perpendicularly to the SAF layer and its effect is experienced only by the top-layer of the SAF. The current-field state diagram obtained exhibits three different behaviors: i) an in-plane stable state corresponding to the parallel or orthogonal alignment of the two SAF layers for low current densities; ii) an incoherent dynamic state for large current densities; iii) a steady out-of-plane magnetization precession of the two SAF layers for intermediate current densities. The current-field range of these steady state excitations is much larger than that obtained for a single free layer spin-torque oscillator and thus more attractive for applications.

(Received November 15, 2010; accepted December 8, 2010)

*Keywords:* Nanomaterials; Numerical simulations; Micromagnetism

### 1. Introduction

Development of multimedia lead to an exponential growth in the demand for electronic devices with high frequency performances that are multistandard, multiband and have a dynamic allocation of frequency. These attributes of future telecommunications applications are difficult to achieve using traditional oscillators, like a LC resonant circuit. An elegant solution is to use a new type of high frequency oscillators whose operation is based on the effects of spintronics (spin transfer torque) [1,2] in nanostructured magnetic devices. There are two types of geometries which have been analysed experimentally and numerically: nanocontact [3-6] and nanopillar [7-22]. A "classical" nanopillar spin-torque oscillator consist of two ferromagnetic layers, a current polarizer (POL) and a free layer (FL) separated by a non-magnetic layer. Up to now different configurations have been studied combining two in-plane magnetized layers [7-10], a perpendicular polarizer and an in-plane free-layer [12-17] or more complex geometries with a SAF structure as polarizer or free layer [18, 20-22]. The spintorque oscillator analyzed here consists in an out-of-plane magnetized polarizer and a SAF structure separated by a Ru nonmagnetic layer (Fig. 1). A SAF is a Ruderman-Kittel-Kasuya-Yosida (RKKY) exchange-coupled two layer system [the top-layer (TL) and the bottom layer (BL)]. The nonmagnetic spacer has a thickness adapted to provide an anti-ferromagnetic alignment in zero applied magnetic field.

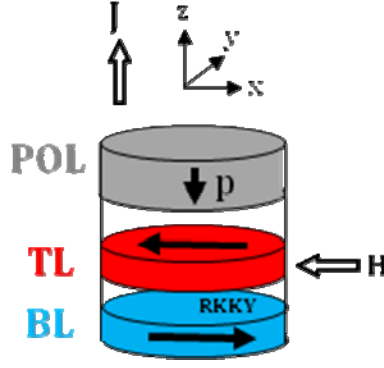


Fig 1: Schematics of the perpendicular polarizer planar SAF free layer oscillator. POL – polarizer, TL – top layer, BL – bottom layer

Testing of this specific perpendicular polarizer structure is realized for magnetic fields applied in-plane and currents injected perpendicular to the plane ( $xOy$ ). Furthermore we assume that the external field  $\mathbf{H}_{\text{app}}$  acts on both layers of the SAF, while the out-of-plane polarized current  $J$  operates only on the TL. The polarizer magnetization is fixed parallel to the  $Oz$  direction. The paper is organized as follows: the model and the numerical approach used in simulations are described in section II. In section III we present the calculated current-field state diagram for the perpendicular polarizer - SAF free layer oscillator for increasing current density. Section IV concludes on the results.

## 2. Macrospin model for the magnetization dynamics

The simulations are carried out by solving the Landau-Lifshitz-Gilbert [23] equation enhanced by the Slonewski's spintorque term [1] (abridged LLGS in this paper) in the single spin approximation:

$$\frac{\partial \mathbf{M}^i}{\partial t} = -\gamma_0 (\mathbf{M}^i \times \mathbf{H}_{\text{eff}}^i) + \frac{\alpha}{M_s^i} \left( \mathbf{M}^i \times \frac{\partial \mathbf{M}^i}{\partial t} \right) - \frac{\gamma_0 a_J^i}{M_s^i} \left[ \mathbf{M}^i \times (\mathbf{M}^i \times \mathbf{P}^i) \right], \quad i = TL, BL \quad (1)$$

Here  $\gamma_0 = \mu_0 \gamma$  is the gyromagnetic factor multiplied by  $\mu_0$ - vacuum permeability ( $\mu_0 = 4\pi \cdot 10^{-7} \text{ N/A}^2$ ),  $\alpha$  the Gilbert damping parameter and  $M_s$  the saturation magnetization of layer  $i$ .  $\mathbf{P}$  is the unitary spin polarization vector, which is parallel to the polarizer magnetization and  $a_j$  represents the amplitude of the spin-torque term, given by:

$$a_j = \frac{\hbar}{2e\mu_0 M_s t} g(\eta, \theta) J \quad (2)$$

with  $\hbar$  Planck's constant,  $e$  the negative electron charge,  $\mu_0$  the magnetic permeability in vacuum,  $t$  the thickness of the free layer and  $J$  the density of the injected current. The prefactor  $g(\eta, \theta)$  is the angular dependent spin polarization efficiency which is a function of the spin polarization  $\eta$  and the angle  $\theta$  between the magnetization  $\mathbf{M}$  and the spin polarization vector  $\mathbf{P}$ . According to the ref. [1] its expression is:

$$g(\eta, \theta) = \left[ -4 + \frac{1}{4} \frac{(1+\eta)^3}{\eta^{3/2}} \left( 3 + \mathbf{P} \cdot \frac{\mathbf{M}}{M_s} \right) \right]^{-1} \quad (3)$$

The effective field  $\mathbf{H}_{\text{eff}}$  regroups the externally applied field  $\mathbf{H}_{\text{app}}$ , the magnetocrystalline anisotropy field  $\mathbf{H}_{\text{anis}}$ , the demagnetizing field  $\mathbf{H}_{\text{D}}$  and the RKKY type coupling field  $\mathbf{H}_{\text{RKKY}}$ :

$$\mathbf{H}_{\text{eff}} = \mathbf{H}_{\text{app}} + \mathbf{H}_{\text{anis}} + \mathbf{H}_{\text{D}} + \mathbf{H}_{\text{RKKY}} \quad (4)$$

The external field  $\mathbf{H}_{\text{app}}$  is oriented in-plane along the Ox direction (Fig. 1), which is also the direction of the uniaxial easy axis giving rise to the magnetocrystalline anisotropy field  $\mathbf{H}_{\text{anis}} = \frac{2K_u}{\mu_0 M_s^2} (\mathbf{u}_x \cdot \mathbf{M}) \mathbf{u}_x$ . The magnetization of the sample is assumed to be uniform (macrospin approach) and the demagnetizing field  $\mathbf{H}_{\text{D}}$  is estimated by using the demagnetizing tensor  $\overline{\overline{N}} = (N_{xx}, N_{yy}, N_{zz})$ ,  $\mathbf{H}_{\text{D}} = -\overline{\overline{N}}\mathbf{M}$ , according to the ref. [24].

The LLGS equation is solved simultaneously for both layers of the SAF, under the assumption that the spintorque acts only on the TL ( $a_j^{\text{BL}} = 0$ ) since the spacer (Ru in our sample) is well-known as a high depolarizer material. The RKKY type coupling field corresponding to the TL,  $\mathbf{H}_{\text{RKKY}}^{\text{TL}}$ , respectively to the BL,  $\mathbf{H}_{\text{RKKY}}^{\text{BL}}$ , are calculated as follows:

$$\mathbf{H}_{\text{RKKY}}^{\text{TL}} = J_{\text{RKKY}} \frac{\mathbf{m}^{\text{BL}}}{t_{\text{TL}} \mu_0 M_s^{\text{TL}}} \quad (5)$$

$$\mathbf{H}_{\text{RKKY}}^{\text{BL}} = J_{\text{RKKY}} \frac{\mathbf{m}^{\text{TL}}}{t_{\text{BL}} \mu_0 M_s^{\text{BL}}} \quad (6)$$

The  $J_{\text{RKKY}}$  is the bilinear coupling energy which quantifies the RKKY coupling strength between the TL and BL of the SAF [25-27]. It is noted that for the parameters studied here (see Table 1) the SAF structure is almost compensated (i.e. the product between the saturation magnetization and the thickness is almost the same for both layers). Numerically the LLGS equation is solved for both layers simultaneously by using a predictor-corrector Heun scheme [28]. The integration time step was  $1fs$  while the total integration time varied from  $80ns$  up to  $200ns$  according to the convergence speed of the numerical solution. For the injected spin current and magnetic applied field steps we considered a rise time of  $2ns$ . The simulations were carried out at  $0K$  temperature.

Table 1: Parameters used in the simulations

Parameters	BL	TL
surface (nm <sup>2</sup> )	70×60	70×60
thickness (nm)	2.5	3.0
M <sub>S</sub> (kA/m)	1600	1340
K <sub>u</sub> (J/m <sup>3</sup> )	8000 // Ox	6700 // Ox
N <sub>xx</sub> , N <sub>yy</sub> , N <sub>zz</sub>	0.045, 0.053, 0.901	0.051, 0.060, 0.887
α	0.02	0.02
η	-	0.3
(P <sub>x</sub> , P <sub>y</sub> , P <sub>z</sub> )	-	(0, 0, -1)
t <sub>spacer</sub> (nm)	0.8	0.8
J <sub>RKKY</sub> (mJ/m <sup>2</sup> )	-1	-1

### 3. Current-field state diagram

For a perpendicular polarizer planar single free layer spintorque oscillator the LLGS macrospin simulations reveal three states of the magnetization as a function of the in-plane applied field and out-of-plane polarized current [14,16].

Fig. 2a shows the current-field diagram of states for the magnetization of a free layer having physical and geometrical proprieties identical to those of the TL. These states are the result of the competition between the spintorque and the damping torque which acts on the free-layer magnetization. Thus, for small values of the current density  $J$  the spintorque, which tends to bring the free-layer magnetization out-of-plane, is not strong enough to induce any dynamics and the magnetization remains in the plane  $xOy$ . This is the in-plane-stable state (IPS). It is noted that the magnetization is tilted with respect to the uniaxial easy axis at an angle which increases with increasing applied current. For large values of  $J$ , the spintorque proportional to  $J$ , stabilizes the magnetization out-of-plane, parallel to the  $Oz$  axis. This stable state is called out-of-plane stable state (OPS). We remark that full micromagnetic simulations reveal that this state is in fact a vortex state [15]. Finally, for intermediate values of current and field, the spintorque equilibrates the

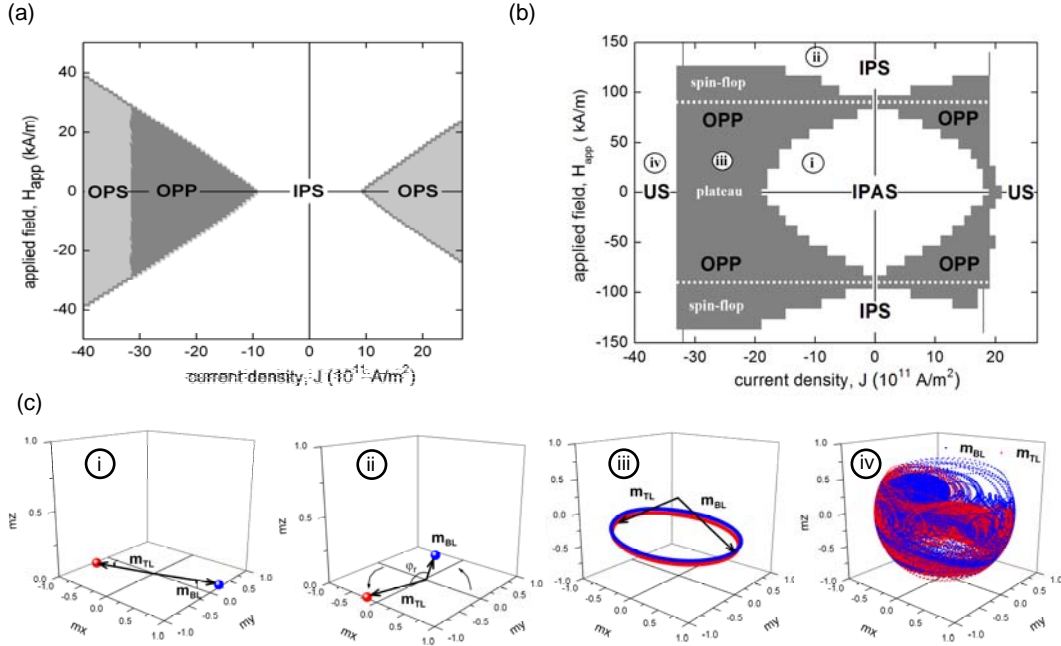


Fig. 2: (a) Diagram of states for the perpendicular polarizer in-plane single free-layer oscillator structure. (b) Diagram of states for the perpendicular polarizer SAF free-layer oscillator structure. (c) Equilibrium states and trajectories on the TL and BL magnetizations corresponding to different regions on the diagram from case b): (i) equilibrium state in the in-plane antiparallel state (IPAS) for  $H_{app}=30$  kA/m and  $J=-10 \cdot 10^{11}$  A/m<sup>2</sup>, (ii) equilibrium state in the in-plane stable state (IPS) for  $H_{app}=130$  kA/m and  $J=-10 \cdot 10^{11}$  A/m<sup>2</sup>, (iii) trajectories in the out-of-plane precession state (OPP) for  $H_{app}=30$  kA/m and  $J=-25 \cdot 10^{11}$  A/m<sup>2</sup> and (iv) trajectories in the unstable state (US) for  $H_{app}=30$  kA/m and  $J=-35 \cdot 10^{11}$  A/m<sup>2</sup>.

damping torque and the free-layer magnetization executes precessions around the out-of-plane axis,  $Oz$ . We obtain a dynamical state, called out-of-plane precession state (OPP) which appears in a triangular shaped region in the current-field diagram. Here again we notice that the full micromagnetic simulations reveal that in the OPP region two types of magnetization distributions exist: a single-spin-like pattern, for small values of current and a more complex pattern with two regions of the layer where the magnetization has a strong out-of-plane component immersed in an in-plane magnetization configuration [15]. It has been demonstrated experimentally [13] and theoretically that in the first case the oscillation frequency increases with increasing current, while in the second one the frequency decreases with increasing current. This second counterintuitive behavior is due to the fact that the dipolar stray field emanating from the out-of-plane regions diminishes the mean out-of-plane magnetization component in the other part of the layer, leading to a reduction of the oscillation frequency.

In order to avoid the formation of this non-uniform configuration, in the present paper we propose to use a free-layer exchanged coupled with another layer forming an SAF. The current-field diagram of states for this perpendicular polarizer - SAF free layer spintorque oscillator is presented in Fig. 2b. In the absence of the spin-polarized current (under the action of the in-plane applied magnetic field only), the SAF reveals three stable configurations of the magnetizations [29] as follows:

a) the *plateau region* where the TL and BL magnetizations are antiparallel aligned to each other and parallel with the in-plane easy axis Ox. This antiparallel configuration appears when the applied field module is less than a certain value, named spin-flip field  $\mathbf{H}_{\text{SF}}$ , equal to 90kA/m for our studies.

b) the *spin-flop region* where both layers of the SAF rotate progressively in-plane toward the increasing applied field direction (Ox). This region is obtained for  $|\mathbf{H}_{\text{SF}}| < |\mathbf{H}_{\text{app}}| < |\mathbf{H}_{\text{SAT}}|$ , where  $\mathbf{H}_{\text{SAT}}$  is called saturation field, equal to 380kA/m for our studies.

c) the *saturation region* where the TL and BL magnetization are both aligned parallel with the applied field. This behavior is obtained for  $|\mathbf{H}_{\text{app}}| > |\mathbf{H}_{\text{SAT}}|$ .

When the injected current is taken into account different magnetization configurations are obtained. In the plateau region and for densities of current varying from  $19 \cdot 10^{10} \text{ A/m}^2$  for zero applied field to  $0.5 \cdot 10^{10} \text{ A/m}^2$  for the spin-flop field an in-plane antiparallel stable state (denoted IPAS) stabilizes (Fig. 2b). Comparing with the initial configuration ( $\parallel$  Ox direction), the magnetizations of the two SAF layers rotate in-plane (xOy) in the counterclockwise sense for positive current densities (Fig. 2c(i)) and in a clockwise sense for negative current densities. In addition, we remark that their perfect mutual antiparallel alignment characteristic to the plateau region in the absence of the spinpolarized current is slightly altered. For instance, for  $H_{\text{app}} = -30 \text{ kA/m}$  the relative angle between the TL and BL magnetizations ( $\varphi_r$ ) varies from  $180^\circ$  to  $172^\circ$  depending on J. The rotation can be explained as in the single layer spintorque oscillator case, when the spintorque pushing the TL magnetization out-of-plane is balanced by the precession torque, which is nonzero only if the TL magnetization is not parallel with the easy axis. In contrast, for constant current density  $\varphi_r$  remains the unchanged. When the applied field increases to a value above  $\mathbf{H}_{\text{SF}}$ , the angle  $\varphi_r$  evolves gradually from approximately  $180^\circ$  to  $0^\circ$  but the magnetizations of the two SAF layers remains in-plane. We simply note this in-plane stable state, IPS (Fig. 2c(ii)).

The most interesting result revealed by the numerical simulations is the dynamical state represented by the grey color on the diagram of Fig. 2b, where the TL magnetization oscillates around the energy maximum. In this region, the spintorque that pushes the TL magnetization out-of-plane balances in average the damping torque, which drags the TL magnetization in-plane. Thus an out-of-plane precession state (OPP) stabilizes. Even if the spinpolarized current acts only on the TL, due to the exchange coupling the BL magnetization oscillates as well. An example of the magnetization trajectories is presented on the Fig. 2c(iii). It is observed that both oscillations take place in the z-plane of the same sign (+Oz for  $J > 0$  and -Oz for  $J < 0$ ) and have more or less the same amplitude. Nevertheless due to the antiferromagnetic coupling, the angle of the TL and BL magnetizations remains at a maximum value along the trajectory. For stronger densities of current ( $J < -31 \cdot 10^{10} \text{ A/m}^2$  for negatives J and  $J > 19 \cdot 10^{10} \text{ A/m}^2$  for positives J) the OPP state becomes unstable and the TL and BL magnetizations describe non-periodic oscillations (Fig. 2c(iv)). This state is denoted unstable state (US). While for an out-of-plane polarizer- single in-plane free-layer oscillator the separation between the OPP and OPS states is a straight line [14], for the SAF free layer oscillator the limit between the OPP and US states is not clearly defined. For this reason we have considered in Fig. 2b the lowest current density generating an unstable state as a function of the externally applied field to mark the beginning of the US. It is noted also that the transition towards the US state passes by a process of a period doubling of the trajectory. Moreover, we remark that for very large current densities the TL magnetization reaches an out-of-plane stable state ( $\mathbf{M}^{\text{TL}} \parallel \text{Oz}$ ), while the BL remains in-plane.

#### 4. Conclusion

In conclusion we have presented the macrospin state diagram of an original nanoscillator structure including an out-of-plane magnetized polarizer and an antiferromagnetic exchanged coupled two layers system (SAF). The top layer of the SAF is free to move under the action of the perpendicular spin-polarized current and in-plane applied magnetic field, while the bottom layer feels only the effects of the field. Comparing with a perpendicular polarizer-single in-plane free-layer oscillator this SAF –free layer oscillator presents a significantly larger dynamical OPP zone (of interest for the applications) but reveal also a more complex behavior for important densities of current.

#### Acknowledgements

This work was supported by CNCSIS-UEFISCU, project number 10654, PNII-RU- TE-77/2010 and by the French national research agency (ANR) through ANR-09-NANO-037 and the Carnot-RF project and Nano2012 convention.

#### References

- [1] J. C. Slonczewski, *J. Magn. Magn. Mater.* 159, L1 (1996); J. C. Slonczewski, *J. Magn. Magn. Mater.* 195, 261 (1999).
- [2] L. Berger, *Phys. Rev. B* 54, 9353 (1996).
- [3] W. H. Rippard, M. R. Pufall, S. Kaka, T. J. Silva, S. E. Russek, *Phys. Rev. B* 70, 100406 (2004).
- [4] W. H. Rippard, M. R. Pufall, S. Kaka, S. E. Russek, and T. J. Silva, *Phys. Rev. Lett.* 92, 027201 (2004).
- [5] W.H. Rippard, M.R. Pufall, S. Kaka, T.J. Silva, S.E. Russek, and J.A. Katine, *Phys. Rev. Lett.* 95, 067203 (2005).
- [6] F.B. Mancoff, N.D. Rizzo, B.N. Engel, and S. Tehrani, *Nature* 437, 7057 (2005).
- [7] S.I. Kiselev, J.C. Sankey, I.N. Krivorotov, N.C. Emley, R.J. Schoelkopf, R.A. Buhrman, and D.C. Ralph, *Nature* 425, 380 (2003).
- [8] A. Tulapurkar, Y. Suzuki, A. Fukushima, H. Kubota, H. Maehara, K. Tsunekawa, D.D. Djayaprawira, N. Watanabe, and S. Yuasa, *Nature* 438, 339 (2005).
- [9] O. Boulle, V. Cros, J. Grollier, L.G. Pereira, C. Deranlot, F. Petroff, G. Faini, J. Barnas, and A. Fert, *Nat. Phys.* 3, 492 (2007).
- [10] B. Georges, J. Grollier, M. Darques, V. Cros, C. Deranlot, B. Marcilhac, G. Faini, and A. Fert, *Phys. Rev. Lett.* 101, 017201 (2008).
- [11] H. Morise and S. Nakamura, *Phys. Rev. B* 71, 014439 (2005).
- [12] K. J. Lee, O. Redon, and B. Dieny, *Appl. Phys. Lett.* 86, 022505 (2005).
- [13] W. Jin, Y. Liu, and H. Chen, *IEEE Trans. Magn.* 42, 2682 (2006).
- [14] D. Houssameddine, U. Ebels, B. Delaet, B. Rodmacq, I. Firastrau, F. Ponthenier, M. Brunet, C. Thirion, J.P. Michel, L. Prejbeanu-Buda, M.C. Cyrille, O. Redon, and B. Dieny, *Nat. Mat.* 6, 447 (2007).
- [15] I. Firastrau, U. Ebels, L. D. Buda-Prejbeanu, J. C. Toussaint, C. Thirion, and B. Dieny, *J. Magn. Magn. Mater.* 310, 2029 (2007).
- [16] I. Firastrau, D. Gusakova, D. Houssameddine, U. Ebels, M.C. Cyrille, B. Delaet, B. Dieny, O. Redon, J.C. Toussaint, and L.D. Buda-Prejbeanu, *Phys. Rev. B* 78, 024437 (2008).
- [17] U. Ebels, D. Houssameddine, I. Firastrau, D. Gusakova, C. Thirion, B. Dieny, and L.D. Buda-Prejbeanu, *Phys. Rev. B* 78, 024436 (2008).
- [18] D. Gusakova, D. Houssameddine, U. Ebels, B. Dieny, L. Buda-Prejbeanu, M.C. Cyrille, and B. Delaet, *Phys. Rev. B* 79, 104406 (2009).
- [19] Q. Mistral, J. V. Kim, T. Devolder, P. Crozat, C. Chappert, J. A. Katine, M. J. Carey, and K. Ito, *Appl. Phys. Lett.* 88, 192507 (2006).

- [20] A. Deac, A. Fukushima, H. Kubota, H. Maehara, Y. Suzuki, S. Yuasa, Y. Nagamine, K. Tsunekawa, D. Djayaprawira, and N. Watanabe, *Nat. Phys.* **4**, 803 (2008).
- [21] A.V. Nazarov, K. Nikolaev, Z. Gao, H. Cho, and D. Song. Microwave generation in MgO magnetic tunnel junctions due to spin transfer effects (invited). in *Proceedings of the 52<sup>nd</sup> Annual Conference on Magnetism and Magnetic Materials*. 2008. Tampa, Florida (USA): AIP.
- [22] D. Houssameddine, S.H. Florez, J.A. Katine, J.P. Michel, U. Ebels, D. Mauri, O. Ozatay, B. Delaet, B. Viala, L. Folks, B.D. Terris, and M.C. Cyrille, *App. Phys. Lett.* **93**, 022505 (2008).
- [23] L. D. Landau and E. Lifshitz, *Phys. Z. Sowjetunion* **8**, 153 (1935).
- [24] A. Hubert, R. Schaffer, *Magnetic Domains*, Springer-Verlang (1998).
- [25] S. S. P. Parkin, N. More, and K. P. Roche, *Phys. Rev. Lett.* **64**, 2304 (1990); J. Unguris, R. J. Celotta, and D. T. Pierce, *J. Appl. Phys.* **75**, 6437 (1994); P. Bruno, *J. Phys. Condes. Matter* **11**, 9403 (1999).
- [26] Z. Zhang, L. Zhou, P. E. Wigen, and K. Ounadjela, *Phys. Rev. B* **50**, 6094 (1994).
- [27] J. Z. Sun *Phys. Rev. B* **62**, 570 (2002).
- [28] J. L. Garcia-Palacios and F. J. Lazaro, *Phys. Rev. B.* **58**, 14937 (1998).
- [29] B. Dieny, M. Li, C. Horng, K. Ju, *J. Appl. Phys.* **87**, 3415 (2000).